

Refilling characteristics of high frequency piezo driven ink jet print heads

J. Frits Dijkstra, Physics of Fluids (Chair Innovative Biomedical Applications of Inkjet Technology) and J.M. Burgers Centre Research School for Fluid Dynamics, Faculty Science and Technology, University of Twente, Enschede, The Netherlands

Abstract

A piezo driven ink jet print head is in principle an open microfluidic system, there are no valves that control the direction of the flow. In order to avoid flooding of the nozzle plate at nozzle level a small under-pressure is maintained. In equilibrium the meniscus of the ink is retracted and pinned to the rim of the nozzle. This equilibrium is controlled by the surface tension of the ink and the setting of under-pressure controller. Operated at low frequencies, after droplet formation, there is ample time for the ink to return to the equilibrium state and to be ready for the next firing of a droplet. Driven at higher frequencies, in between droplets, there is no time to return to the equilibrium state and other mechanisms for refilling come into view. When the meniscus has retracted in the nozzle, the next pressure pulse needs to accelerate a relatively small amount of ink. Moreover the viscous drag in a partly filled nozzle is less compared to a completely filled nozzle. With a constant surface tension pressure, the Washburn equation learns that the refilling speed of a partly filled nozzle increases with decreasing filling of the nozzle. Both effects are supposed to cause that a print head driven at high frequency delivers enough fluid to nozzle to maintain droplet emission. In this paper this theoretical framework is extended by taken into account:

- Droplet formation on the dynamics of the fluid motion,
- Change of droplet volume at high frequencies,
- Inertia effects due to the variable mass in the nozzle.

A complete non-linear analysis will be outlined including:

- Limitation of the capillary pressure; only close to the nozzle the capillary pressure becomes a linear function of the meniscus displacement, otherwise it is a constant,
- The dependence of the viscous drag on the filling of the nozzle,
- The effects of droplet formation,
- Inertia effects due to the variable mass in the nozzle.

Calculations will be performed for a sample pump of which the dimensions are representative for a standard print head. Two inks will be investigated one with a viscosity of 0.01 Pa.s and another with a low viscosity equal to 0.002 Pa.s.

The non-linear analysis will reveal many details of the fluid dynamics of the ink in a print head, including effects of surface tension, viscosity, droplet formation, pulse shape and repeat rate.

Introduction

A piezo driven ink jet print head is in principle an open microfluidic system, there are no valves that control the direction of the flow. In order to avoid flooding of the nozzle plate at nozzle level a small under-pressure is maintained. In equilibrium the meniscus of the ink is retracted slightly and pinned to the rim of the nozzle. This equilibrium is controlled by the surface tension of the ink and the setting of the under-pressure controller. Operated at low frequencies, after droplet

formation, there is ample time for the ink to return to the equilibrium state and to be ready for the next firing of a droplet. Driven at higher frequencies, in between droplets, there is no time to return to the equilibrium state and other mechanisms for refilling come into view. Wijshoff [1,2,3] has described two mechanisms depending on the filling of the nozzle. When the meniscus has retracted in the nozzle, the next pressure pulse needs to accelerate a relatively small amount of ink. Moreover the viscous drag in a partly filled nozzle is less compared to a completely filled nozzle. With a constant surface tension pressure, the Washburn equation learns that the refilling speed of a partly filled nozzle increases with decreasing filling of the nozzle [4]. Both effects are supposed to cause that a print head driven at high frequency deliver enough fluid to nozzle to maintain droplet emission. In this paper the theoretical framework of Wijshoff is extended by taken into account:

- Droplet formation on the dynamics of the fluid motion,
- Change of droplet volume at high frequencies,
- Inertia effects due to the variable mass in the nozzle.

First an estimate on the surface tension driven refilling is derived giving a kind of upper bound for the driving frequency. As for high frequency jetting the meniscus at the moment of firing may be retracted far beyond the equilibrium position given by the under-pressure controller, the droplet volume and droplet speed as functions of the meniscus position will be derived. Finally a complete non-linear analysis will be outlined including:

- Limitation of the capillary pressure; only close to the nozzle the capillary pressure becomes a linear function of the meniscus displacement, otherwise it is a constant,
- The dependence of the viscous drag on the filling of the nozzle,
- The effects of droplet formation,
- Inertia effects due to the variable mass in the nozzle.

Calculations will be performed for a sample pump of which the dimensions are representative for a standard print head. Two inks will be investigated one with a viscosity of 0.01 Pa.s and another with a low viscosity equal to 0.002 Pa.s.

The non-linear analysis will reveal many details of the fluid dynamics of the ink in a print head, including effects of surface tension, viscosity, droplet formation, pulse shape and repeat rate.

Sample print head

In the analysis outlined in this paper we use a sample print head as depicted in figure 1.

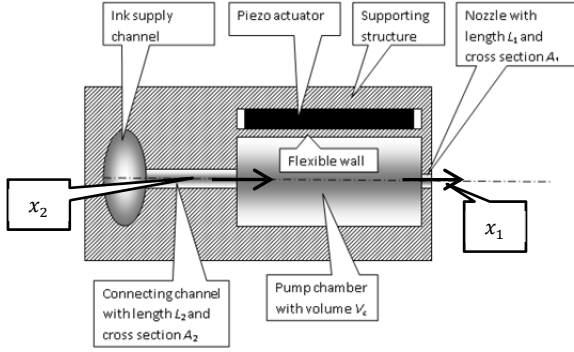


Figure 1 Schematic of a Helmholtz type of print head; note the definitions of the fluid motion in the throttle x_2 and the fluid motion in the nozzle x_1

The dimensions are:

- Volume pump chamber $V_c = 2 \cdot 10^{-10} \text{ m}^3$ (length 10 mm, cross-section 200 by $100 \mu\text{m}^2$),
- Nozzle length $L_1 = 75 \mu\text{m}$, radius $R_1 = 15 \mu\text{m}$, ($A_1 = 707 \mu\text{m}^2$),
- Throttle length $L_2 = 500 \mu\text{m}$, cross-section 40 by $40 \mu\text{m}^2$ ($A_2 = 1600 \mu\text{m}^2$).

The ink is characterized by its surface tension $\gamma = 0.05 \text{ N/m}$, viscosity $\mu = 0.01 \text{ Pa.s}$ and density $\rho = 1000 \text{ kg/m}^3$. Another ink will be considered as well, with a viscosity of 0.002 Pa.s .

The wave speed in the system (or the speed of sound corrected for the compliance of the environment) equals $c = 1200 \text{ m/s}$.

The pulse form used for driving the print has a leading edge step of $0.1 \mu\text{s}$, the duration of the pulse equals $3.4 \mu\text{s}$. In order to keep the pressure in the pump chamber above zero (no vacuum) the pulse is switched off in a linear ramp during $25 \mu\text{s}$. The volume displacement of actuator is chosen equal to 40 pl .

Surface tension driven refilling

The fluid retracts in the nozzle after firing a droplet and refilling starts due to surface tension. The situation is visualised in figure 2. The droplet has separated and the meniscus has retracted inside the nozzle.

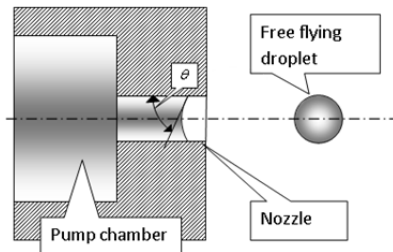


Figure 2 Situation after droplet has separated from the fluid inside the nozzle. The meniscus has retracted.

The capillary pressure is given by [5]:

$$p_{cap} = \frac{2\gamma \cos \theta}{R_1} \quad (1)$$

A simple estimate can be found for the calculation the surface tension driven filling time based by combining Hagen-Poiseuille law [6] and the capillary under-pressure given above (1) into a modified Washburn equation [4]:

$$\tau_\gamma = \frac{4\mu R_1}{\gamma \pi \cos \theta} \left[\left(\frac{L_1}{R_1^4} + \frac{L_2}{R_2^2} \right) V - \frac{1}{4} \frac{\pi}{R_1^2} \left(\frac{V}{\pi R_1^2} \right)^2 \right] \quad (2)$$

where θ is the contact angle of the ink on the inside surface of the nozzle (usually in the nozzle θ is small and taken equal to zero) and V the volume of the droplet. Note that for refilling the dimensions of the throttle are included in the time involved in refilling due to surface tension. Capillary filling is only active when the fluid inside the nozzle is behind the nozzle front. At the moment the liquid approaches the rim of the nozzle, filling due to capillary pressure starts to slow down until the meniscus is flat or given by the under-pressure control of the print head [7].

Droplet volume and speed

To describe droplet formation, in particular the conditions to be met for droplet emission, droplet volume and speed and the existence of satellites the approach developed in [9,10,11, see also 12] has been followed.

In case of an under-pressure or at the moment a next pulse is applied to the print head the meniscus has retracted over a certain distance x_0 . When the print head is idling, this position must be stable limiting the set under-pressure to:

$$p_{under-pressure} < \frac{2\gamma}{R_1} \cos \theta \quad (3)$$

A necessary condition for droplet formation is met as at the same time the velocity of the fluid inside the nozzle is positive and the meniscus position has passed the nozzle front. In case of positive pulsing (directly after the leading edge of the pulse the fluid starts to move out of the nozzle) the velocity and the fluid displacement are given by (note that t starts with the leading edge of the pulse, v_{max} denotes the amplitude of the mean velocity of the fluid in the nozzle):

$$\dot{x}_1(t) = v_{max} \sin \omega_0 t \quad (4)$$

$$x_1(t) = -x_0 + \frac{v_{max}}{\omega_0} (1 - \cos \omega_0 t)$$

where x_0 measures the distance of the meniscus from the nozzle front at the moment the velocity changes sign from negative to positive. In case of no under-pressure control for low frequency jetting x_0 equals the volume of the droplet V divided by the surface area of the nozzle A_1 . Otherwise x_0 depends on the motion of the meniscus caused by pulsing. The acoustic properties of the print head are put in the angular frequency ω_0 . For a Helmholtz type of print head the high angular Helmholtz frequency and the low angular frequency of the surface tension driven slosh mode are given by [7]:

$$\omega_0 = c \sqrt{\frac{1}{V_c} \left(\frac{A_1}{L_1} + \frac{A_2}{L_2} \right)} \quad (5)$$

$$\omega_{slosh} = \sqrt{\frac{8 \gamma}{\pi \rho_0 R_1^4 L_2} \frac{1}{L_2}}$$

(For the sample print head and ink $f_0 = \omega_0/2/\pi = 48$ kHz, $f_{slosh} = \omega_{slosh}/2/\pi = 14.3$ kHz).

The meniscus passes the nozzle front at the moment $t = t_0$ given by:

$$\cos \omega_0 t_0 = 1 - \frac{x_0 \omega_0}{v_{max}} \quad (6)$$

It is assumed that the jet issues from the nozzle like a cylinder with the same cross-sectional dimensions as the nozzle. Then the kinetic energy passing the nozzle front is given by:

$$T(t) = \frac{1}{2} \rho_0 A_1 \int_{t_0}^t v^3(t') dt' \quad (7)$$

The fluid portion outside the nozzle moves as a solid mass of which the kinetic energy is defined by ($t > t_0$):

$$T_d = \frac{1}{2} \rho_0 A_1 x_1(t) v^2(t) \quad (8)$$

During outflow extra free surface is created. As the jet almost moves like a solid cylinder, the increase in surface energy can be expressed as with P_1 the perimeter of the jet ($t > t_0$):

$$W = \gamma P_1 x_1(t) = \gamma 2\pi R_1 x_1(t) \quad (9)$$

The condition for the formation of a droplet is reached as soon as the kinetic energy transported along with the fluid issuing from the nozzle equals the kinetic energy of the cylinder (droplet) plus the extra surface energy:

$$T(t) = T_d + W \quad (10)$$

On substituting the expressions for the different energies given above, this condition becomes:

$$\int_{t_0}^t v(t') \{v^2(t') - v^2(t)\} dt' = \frac{2\gamma P_1}{\rho_0 A_1} x_1(t) \quad (11)$$

It is clear that this condition can only be fulfilled after the velocity has gone through a maximum. Carrying out all the integrations and lowering the type of the equation from cubic to quadratic by factoring out $(1 - \cos \omega_0 t)$ a quadratic equation in $\cos \omega_0 t$ is obtained:

$$2\cos^2 \omega_0 t - \cos \omega_0 t_0 \cos \omega_0 t - \left(\frac{6\gamma P_1}{\rho_0 A_1 v_{max}^2} + \cos^2 \omega_0 t_0 \right) = 0 \quad (12)$$

With solutions:

$$\cos \omega_0 t^* = \frac{1}{4} \cos \omega_0 t_0 \left(1 \pm 3 \sqrt{1 + \frac{16\gamma P_1}{3\rho_0 A_1 (v_{max} \cos \omega_0 t_0)^2}} \right) \quad (13)$$

The negative sign option makes sense in this case because $|\cos \omega_0 t^*| < 1$. As $\cos \omega_0 t^* > -1$, ($\omega_0 t^* > \pi/2$) the velocity amplitude in the nozzle has to be above a threshold value defined by:

$$v_{max} > \sqrt{\frac{6}{2 + \cos \omega_0 t_0 - \cos^2 \omega_0 t_0} \frac{\gamma P_1}{\rho_0 A_1}} \quad (14)$$

The volume of the droplet and the droplet speed, respectively, are given by:

$$V = A_1 x_1(t^*) = A_1 \left[-x_0 + \frac{v_{max}}{\omega_0} (1 - \cos \omega_0 t^*) \right] \quad (15)$$

$$\dot{x}_1(t^*) = v_{max} \sin \omega_0 t^*$$

Figure 3 shows a typical result.

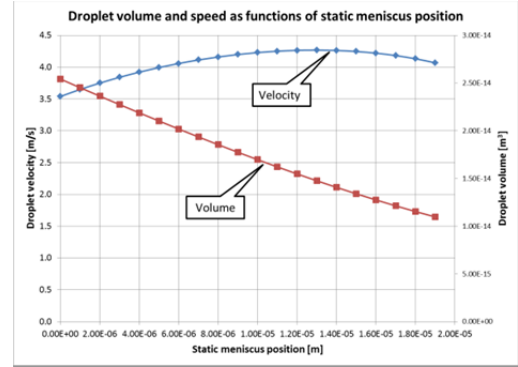


Figure 3 Droplet velocity and volume as functions of the meniscus position (positive inwards) for 6 m/s velocity amplitude in the nozzle. Dimensions print head see sample print head.

Clearly is visible that the droplet volume decreases with increasing meniscus position at the moment of applying the pulse (defined positive inwards, generating instantaneously a positive pressure). As mentioned earlier the static under-pressure must be small, otherwise the nozzle empties itself into the pump chamber and the ink reservoir, and the print head is no longer operational. It will be shown later that the meniscus during high frequency pulsing can be retracted over a larger distance. For a non-retracted meniscus the droplet volume for the example discussed measures 25 pl, to replenish this volume formula (2) learns that $\tau_\gamma = 3.1$ ms, allowing for a repeat rate of 3.25 kHz.

During jetting at higher frequencies the meniscus retracts further and further, the print head delivers smaller but faster droplets. Half the droplet volume means a twofold increase in

jetting frequency. This mechanism explains, at least qualitatively, why usually a print head can run at higher frequencies than predicted by surface tension driven refilling based on the low frequency droplet volume. It adapts the volume of the droplets emitted.

Non-linear analysis of print head in the time domain

The Helmholtz resonator type of print head is the simplest configuration to develop a non-linear description of its action. This analysis contains the following ingredients.

Surface tension effects

In the equilibrium situation the fluid at the end of the nozzle forms a meniscus. The solid, fluid and air contact line pins at the rim of the nozzle. The geometric details are depicted in figure 4.

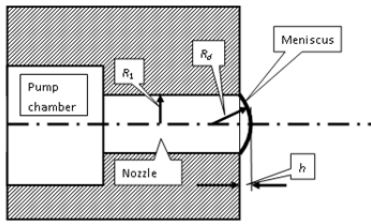


Figure 4 Geometric details of meniscus shape

In case the fluid moves outwards the meniscus is deformed in such a way that the curvature increases and as a consequence the capillary pressure increases as well. The capillary pressure inside the domed meniscus opposes the motion of the fluid column in the nozzle. When the fluid retracts into the nozzle a concave meniscus is formed. The capillary pressure is again opposing the retracting motion of the fluid. The relation between the fluid displacement x_1 , the dome height h and the radius of the nozzle R_1 reads [7]:

$$A_1 x_1 = \frac{1}{6} \pi h (3R_1^2 + h^2) \quad (16)$$

The radius of curvature of the dome R_d follows from (Pythagoras formula):

$$R_d = \frac{R_1^2 + h^2}{2h} \quad (17)$$

With Laplace equation [5] an expression is obtained for the capillary pressure as a function of the fluid displacement x_1 [7]:

$$p_{cap} = \frac{2\gamma}{R_d} \cong \frac{8\pi\gamma}{A_1} x_1 = \frac{8\gamma}{R_1^2} x_1 \quad (18)$$

The approximated expression shows that the pressure depends linearly on the fluid displacement x_1 , like a mechanical spring.

Expression (18) is only valid for small displacements. At the very moment the radius of curvature becomes equal to the radius of the nozzle, the capillary pressure becomes a constant. In case the fluid in the nozzle moves more and more inwards the capillary pressure becomes constant and equal to:

$$p_{cap} = -\frac{2\gamma}{R_1}, x_1 < -\frac{1}{4}R_1 \quad (19)$$

It is assumed that a similar expression holds true for the case that the meniscus moves outwards:

$$p_{cap} = \frac{2\gamma}{R_1}, x_1 > \frac{1}{4}R_1 \quad (20)$$

For the sample print head, this means that expression (18) holds true as long as $|x_1| < 3.75 \mu\text{m}$. When the nozzle front is wetted, the capillary pressure vanishes. The capillary force acting on the fluid in the nozzle is given by:

$$F_{cap} = p_{cap} A_1 \quad (21)$$

Viscous force

Viscosity is opposing the motion of the ink in the nozzle, in terms of force the Hagen Poiseuille relation [6] can be written as (note that this equation holds for nozzle and throttle):

$$F_{viscous} = \Delta p A = \frac{8\mu L}{\pi R^4} Q = 8\pi\mu L \dot{x} \quad (22)$$

In the throttle the length of the fluid column stays constant:

$$F_{viscous,throttle} = 8\pi\mu L_2 \dot{x}_2 \quad (23)$$

In the nozzle the situation is different, for a retracting meniscus the fluid column becomes shorter and consequently the viscous drag will be reduced according to [1,2,3,4]:

$$x_1 < 0, F_{viscous,nozzle} = 8\pi\mu(L_1 + x_1)\dot{x}_1 \quad (24)$$

In case the meniscus is outside the nozzle the fluid column length stays constant:

$$x_1 > 0, F_{viscous,nozzle} = 8\pi\mu L_1 \dot{x}_1 \quad (25)$$

Inertia effects

To model the inertia force the effect of the varying mass in the nozzle must be taken into account. To model this effect the so-called rocket formula is used [13]:

$$m(t) \frac{dx_1}{dt} = u \frac{dm}{dt} + \sum F \quad (26)$$

In terms of rocket science dm/dt is the ejected mass per unit time and u the relative velocity of the ejected gas defined with respect to the rocket. Special attention has to be paid to what happens at the entrance of the nozzle. The Reynolds number of the flow entering the nozzle or leaving the nozzle is about 10-50. This value resembles the cigarette smoker dilemma, he can blow out smoke in the shape of a jet, but he is never able to suck in the jet. Or said otherwise, blowing out generates a jet, the stream

lines are parallel; sucking in generates sink flow, the stream lines are directed towards the mouth in a spherical manner. These two effects are shown in figure 5 for the flow situation close to the entrance of the nozzle seen from the pump chamber.

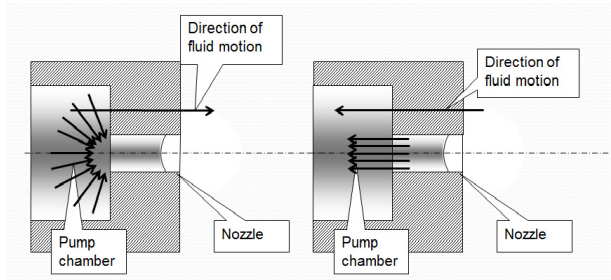


Figure 5 Stream lines close to the nozzle entrance. Left for the case that the flow is towards the nozzle, depicted as sink flow, right the case is depicted that the flow is from the nozzle into the pump chamber, shown as a jet

In case the fluid flows from the nozzle to the pump chamber the jet has the same velocity as the fluid in the nozzle and $u = 0$. There is no thrust. For the sink flow case the component of the impulse parallel to the axis of the nozzle must be calculated (see figure 6)

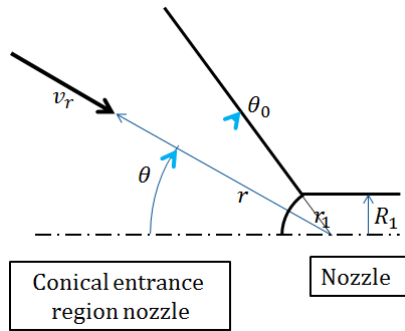


Figure 6 Flow kinematics near the nozzle for the sink flow case. All stream lines are directed towards the nozzle. The entrance region is bounded by a conical surface given by $\theta = \theta_0$. The flow is axisymmetric, the spherical coordinates to define a point in space are θ , ϕ and r . The velocity vector v_r is positive towards the origin. The radius of the nozzle is denoted by R_1 ; the component of the velocity parallel to the axis is evaluated at the spherical surface defined by r_1 .

Sink flow flow kinematics are described by:

$$v_r = \frac{Q}{2\pi r^2(1 - \cos \theta_0)}, \quad Q = A_1 \dot{x}_1 \quad (27)$$

The integrated velocity component parallel to the axis of the nozzle ($r_1 = R_1 / \sin \theta_0$) can be found by evaluation of:

$$\bar{v} = \frac{1}{\pi R_1^2} \int_0^{\theta_0} v_r \cos \theta r_1 d\theta 2\pi r_1 \sin \theta = \frac{1}{2} \dot{x}_1 \frac{\sin^2 \theta_0}{(1 - \cos \theta_0)} \quad (28)$$

Note that the integrated velocity component is towards the nozzle. The ejection speed (relative velocity) defined with respect to the moving fluid in the nozzle follows from:

$$u = (\bar{v} - \dot{x}_1) \quad (29)$$

With limiting cases:

$$\theta_0 = 0, \quad \rightarrow u = 0, \quad \theta_0 = \frac{\pi}{2}, \quad \rightarrow u = -\frac{1}{2} \quad (30)$$

As the mass in nozzle varies with meniscus position the equation of motion in fluid contained in the nozzle reads ($x_1 = 0$ coincides with rim):

$$\rho A_1 (L_1 + x_1) \ddot{x}_1 = u \frac{dm}{dt} + \sum F \quad (31)$$

$\sum F = \text{pressure force} - \text{viscous drag} - \text{surface tension force}$

For $\dot{x}_1 > 0$, $dm/dt > 0$ and $u < 0$, which means that the ‘‘propulsion force’’ is actually negative, like the surface and viscosity related forces. The equation of motion of the fluid moving back and forth through the throttle can be derived following the same lines as above; the only differences are that there is no surface tension force and that the mass is constant:

$$\rho A_2 L_2 \ddot{x}_2 = -p A_2 - 8\pi\mu L_2 \dot{x}_2 \quad (32)$$

The closing relation connecting the fluid motion in the nozzle and the throttle is given by:

$$p = \frac{\rho c^2}{V_c} \Delta V_c, \quad \Delta V_c = A_2 x_2 - A_1 x_1 + \Delta V_{act}(t) \quad (33)$$

This set of equations is solved by first eliminating the pressure p by substitution of the closing relation in the two equations of motion and rewriting the two second order differential equations into four first order differential equations by putting [14]:

$$\frac{dx_1}{dt} = p_1, \quad \frac{dx_2}{dt} = p_2 \quad (34)$$

$$\frac{dp_1}{dt} = F(p_1, x_1, x_2), \quad \frac{dp_2}{dt} = G(p_2, x_1, x_2)$$

This set can be solved from given initial conditions by stepwise integration.

A typical result is shown in figure 7 for the set of initial conditions:

$$t = 0: x_1 = x_2 = p_1 = p_2 = 0 \quad (35)$$

The non-linear calculation will be carried out along with the droplet formation condition derived in the droplet formation section.

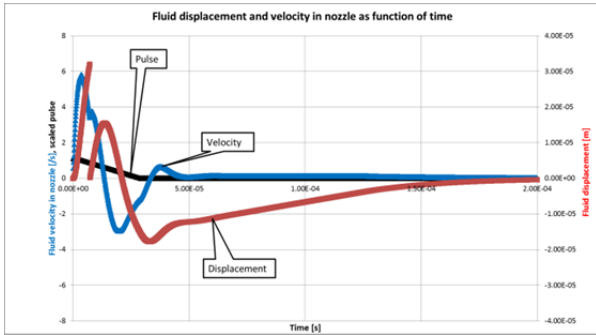


Figure 7 Fluid displacement and velocity in the nozzle for low frequency pulsing ($f_{pulse} = 3.3 \text{ kHz}$) for the sample print head, sample ink ($\gamma = 0.05 \text{ N/m}$, $\mu = 0.01 \text{ Pa}\cdot\text{s}$ and $\rho = 1000 \text{ kg/m}^3$) and sample pulsing ($0.1 \mu\text{s}$ leading edge, $3.4 \mu\text{s}$ pulse duration and $25 \mu\text{s}$ ramp-down time, volume displacement 40 pl) case. The time step used is 10^{-10} s . The droplet formed (see step in fluid displacement) has a volume of 22.7 pl and a velocity of 3.38 m/s

A number of features can be seen:

- Upon droplet formation the meniscus immediately retracts to the zero position and continues to move out because the velocity is still positive.
- Directly after detachment of the droplet the mass involved in the force balance has reduced accordingly, causing the fluid velocity to increase for a short while.
- Because of droplet formation the meniscus retracts over a considerable length, initially refilling takes place at a constant rate driven by the constant capillary under-pressure, at the moment the meniscus has passed the point $x_1 = -R_1/4$, the surface tension force becomes dependent on position and the refilling starts to slow down (first order behavior). It takes indeed about $300 \mu\text{s}$ before the meniscus has reached the equilibrium position.

In figure 8 the pressure in the pump chamber is depicted for the same case as described in the caption of figure 6.

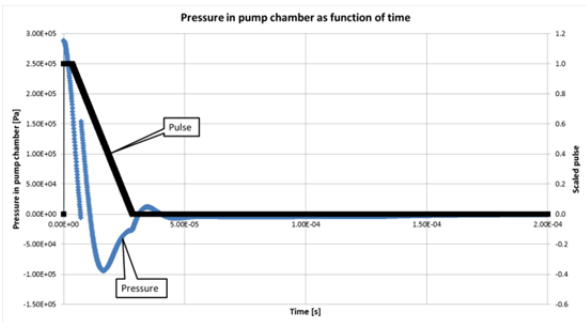


Figure 8 Pressure in pump chamber as function of time for low frequency pulsing ($f_{pulse} = 3.3 \text{ kHz}$) for the sample print head, sample ink ($\gamma = 0.05 \text{ N/m}$, $\mu = 0.01 \text{ Pa}\cdot\text{s}$ and $\rho = 1000 \text{ kg/m}^3$) and sample pulsing ($0.1 \mu\text{s}$ leading edge, $3.4 \mu\text{s}$ pulse duration and $25 \mu\text{s}$ ramp-down time, see black line, and 40 pl actuator displacement). The time step used is 10^{-10} s . Note that the pressure does not reach -1 bar with respect to ambient.

Also in figure 8 the effect of the detachment of the droplet is clearly visible. The pressure does not exceed lower values than -1 bar , which means that cavitation is not occurring and that air entrapment via the nozzle is not likely [15,16,17]. Droplet formation helps to end up with higher positive pressures in the pump chamber resulting in higher droplet velocities and a more stable action of the print head, while at the same time limiting the negative pressure.

The situation in terms of velocity, fluid displacement and droplet formation for driving at a higher frequency (6.67 kHz) is depicted in figure 9.

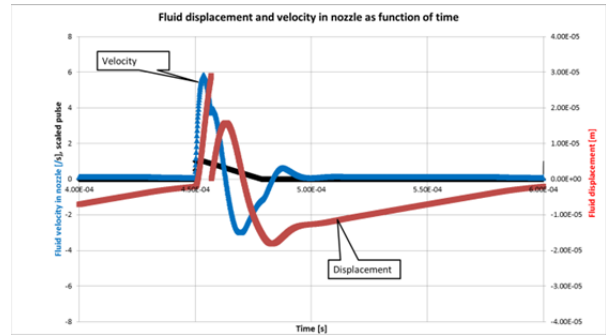


Figure 9 Fluid displacement and velocity in the nozzle for higher frequency pulsing ($f_{pulse} = 6.67 \text{ kHz}$) for the sample print head, sample ink ($\gamma = 0.05 \text{ N/m}$, $\mu = 0.01 \text{ Pa}\cdot\text{s}$ and $\rho = 1000 \text{ kg/m}^3$) and sample pulsing ($0.1 \mu\text{s}$ leading edge, $3.4 \mu\text{s}$ pulse duration and $25 \mu\text{s}$ ramp-down time, volume displacement 40 pl) case. The time step used is 10^{-10} s . The time window is from $400\text{--}600 \mu\text{s}$. The first droplet formed has a volume of 22.7 pl and a velocity of 3.38 m/s , after $450 \mu\text{s}$ (the fourth droplet) the droplet volume has decreased to 21 pl , at the same time the droplet velocity has increased to 3.69 m/s .

The frequency is now so high that the meniscus cannot reach the equilibrium position anymore and the droplet is fired from a retracted meniscus, ending up with a smaller droplet with a higher speed compared to the first droplet. For experimental evidence of the so-called first droplet phenomenon, see [18]. It appears that the frequency can be increased to really high values 20 kHz , see figure 10.

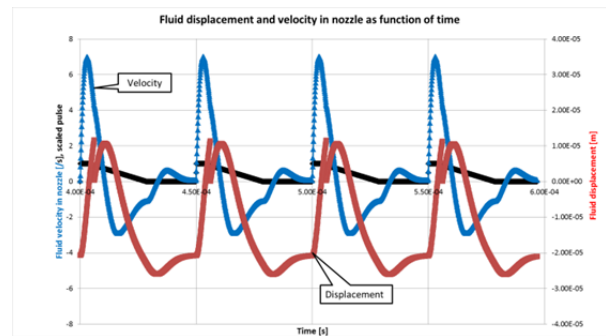


Figure 10 Fluid displacement and velocity in the nozzle for very high frequency pulsing ($f_{pulse} = 20 \text{ kHz}$) for the sample print head, sample ink ($\gamma = 0.05 \text{ N/m}$, $\mu = 0.01 \text{ Pa}\cdot\text{s}$ and $\rho = 1000 \text{ kg/m}^3$) and sample pulsing ($0.1 \mu\text{s}$ leading edge, $3.4 \mu\text{s}$ pulse duration and $25 \mu\text{s}$ ramp-down time, volume displacement 40 pl) case. The time step used is 10^{-10} s . The time frame is from $400\text{--}600 \mu\text{s}$. The first droplet has a volume of 22.7 pl and a velocity of 3.38 m/s , after $550 \mu\text{s}$ (the twelfth droplet) the droplet volume has decreased to a constant value (not dependent on droplet number) of 8 pl , at the same time the droplet velocity has increased to 4.32 m/s .

Figures 11 and 12 show what happens when the ink has a lower viscosity ($0.002 \text{ Pa}\cdot\text{s}$ instead of $0.01 \text{ Pa}\cdot\text{s}$).

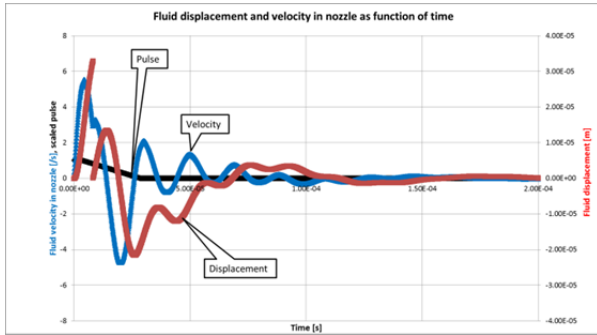


Figure 11 Fluid displacement and velocity in the nozzle for low frequency pulsing ($f_{pulse} = 3.3 \text{ kHz}$) for the sample print head, low viscosity ink ($\gamma = 0.05 \text{ N/m}$, $\mu = 0.002 \text{ Pa}\cdot\text{s}$ and $\rho = 1000 \text{ kg/m}^3$) and adapted pulsing ($0.1 \mu\text{s}$ leading edge, $3.4 \mu\text{s}$ pulse duration and $25 \mu\text{s}$ ramp-down time, volume displacement actuator 24 pl) case. The time step used is 10^{-10} s . The droplet formed (see step in fluid displacement) has a volume of 23.4 pl and a velocity of 2.91 m/s

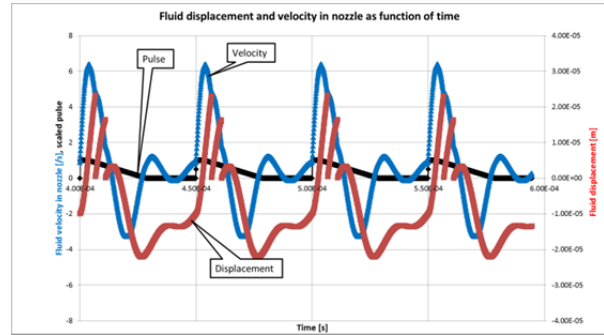


Figure 13 Fluid displacement and velocity in the nozzle for very high frequency pulsing ($f_{pulse} = 20 \text{ kHz}$) for the sample print head, low viscosity ink ($\gamma = 0.05 \text{ N/m}$, $\mu = 0.002 \text{ Pa}\cdot\text{s}$ and $\rho = 1000 \text{ kg/m}^3$) and adapted pulsing ($0.1 \mu\text{s}$ leading edge, $3.4 \mu\text{s}$ pulse duration and $25 \mu\text{s}$ ramp-down time, volume displacement 24 pl) case. The time step used is 10^{-10} s . The time frame is from $400\text{--}600 \mu\text{s}$. The first droplet has a volume of 23.4 pl and a velocity of 2.91 m/s , after $550 \mu\text{s}$ (the twelfth droplet) the droplet volume has increased to a constant value (not dependent on droplet number) of 28.2 pl , at the same time the droplet velocity has increased to 3.54 m/s . The steady state droplet is formed out of two, in the fluid displacement curve there are two steps downward. These two droplets are formed directly after each other and merge to one droplet almost instantaneously.

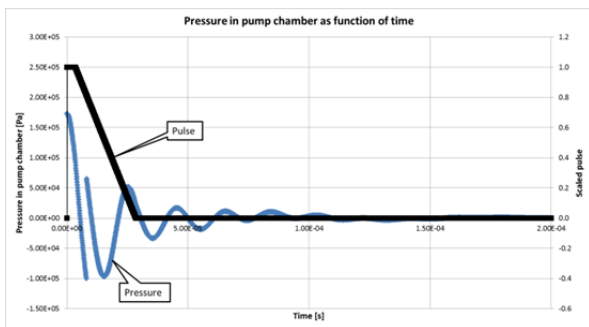


Figure 12 Pressure in pump chamber as function of time for low frequency pulsing ($f_{pulse} = 3.3 \text{ kHz}$) for the sample print head, low viscosity ink ($\gamma = 0.05 \text{ N/m}$, $\mu = 0.002 \text{ Pa}\cdot\text{s}$ and $\rho = 1000 \text{ kg/m}^3$) and adapted pulsing ($0.1 \mu\text{s}$ leading edge, $3.4 \mu\text{s}$ pulse duration and $25 \mu\text{s}$ ramp-down time, see black line, displacement actuator 24 pl) case. The time step used is 10^{-10} s . Note that the pressure does not reach -1 bar with respect to ambient.

Changing the viscosity from $0.01 \text{ Pa}\cdot\text{s}$ to $0.002 \text{ Pa}\cdot\text{s}$ shows some remarkable effects:

- The low-frequency slosh mode oscillation is clearly visible.
- Damping is poor, both for the high frequency Helmholtz oscillations as well as for the low frequency surface tension driven meniscus motion.
- The refilling of the nozzle is much faster, $42\text{--}43 \mu\text{s}$ for the low viscosity case compared to $\sim 300 \mu\text{s}$ for the $0.01 \text{ Pa}\cdot\text{s}$ case. This can be mainly attributed to the decrease in viscosity and partly due the dynamic effects related to the partial filling of the nozzle because of the stronger oscillatory motion [1,2,3].
- The displacement of the actuator has been chosen equal to 24 pl (for the $0.01 \text{ Pa}\cdot\text{s}$ ink 40 pl was needed), in order to keep the negative pressure above than -1 bar . Droplet speed and size are comparable.

Figure 13 shows the behavior of a high frequency driven print head filled with a low viscosity ink. Most clearly is visible that the fast refilling even results in faster and bigger droplets. This is partly due to the fact that the pulsing is almost tuned to the natural timing of the print head. Pulsing starts at the maximum of the velocity.

Discussion and conclusions

The full non-linear analysis of a Helmholtz type print head reveals that dynamic effects associated with partial filling of the nozzle enhance the refilling of the nozzle after release of a droplet [1,2,3]. The difference between the inertia effects linked to outflow or inflow at the entrance of the nozzle seen from the pump chamber reduces this effect, but for low viscosity inks the dynamic refilling is still most clear. This effect can be so strong that at high frequency jetting the droplets are larger and leave the print head at higher speed and/or the nozzle front will be flooded, despite the setting of the under-pressure controller.

Droplet formation reduces the amount of fluid in the nozzle and consequently the pressure waves in the pump chamber. Droplet formation makes it possible to use a larger displacement of the actuator, resulting in a higher positive pressure in the pump chamber leading to a higher droplet velocity and to a more stable operation of the print head.

The pulse shape has chosen such that the leading edge sets the ink in motion, the trailing edge is chosen to ramp down slowly to avoid additional pressure waves that may lead to cavitation and/or entrainment of small air bubbles.

For low viscosity inks the dynamic refilling is so effective that over a broad range of frequencies the print head will function well, in terms of delivering droplets with about constant volume and constant speed even at very high frequencies [19]. For inks with a higher viscosity, however, refilling is much less effective resulting a jetting of droplets with a decreasing volume and higher speed with increasing frequency.

Acknowledgements

The author acknowledges the inspiring and in depth discussions with H. Wijshof of the Technical University of Eindhoven, The Netherlands, J. Snoeijer of the University of Twente, The Netherlands and M. Crankshaw and M. Dorrestijn of XAAR UK.

References

- [1] H. Wijshoff, Structure and Fluid Dynamics in Piezo Printheads, Thesis Eindhoven University of Technology 2008, pp 65-68.
- [2] H. Wijshoff, Physics Reports 491, pp 77-177 (2010).
- [3] H. Wijshoff, Inkjet-based Micromanufacturing, chapter 10, edited by J.G. Korvink, P.J. Smith and D-Y Shin, Wiley-VCH 2012, pp 150-152
- [4] P.G. de Gennes, F. Brochard-Wyart and D. Queré, Capillarity and Wetting Phenomena, Springer 2003, pp 130-131.
- [5] P.G. de Gennes, F. Brochard-Wyart and D. Queré, Capillarity and Wetting Phenomena, Springer 2003, pp 7.
- [6] R.B. Bird, W.E. Stewart and E.N. Lightfoot, Transport Phenomena, Second Edition, Wiley 2002, pp 48-52.
- [7] J.F. Dijkman and A. Pierik, Dynamics of Piezoelectric Print-Heads, Chapter 3 of Inkjet Technology for Digital Fabrication, Edited by I.M. Hutchings and G.D. Martin, Wiley (2013), pp 73.
- [8] J.F. Dijkman, Hydro-acoustics of Piezoelectrically Driven Ink-Jet Print Heads, Flow, Turbulence and Combustion 61, 211-237 (1999)
- [9] J.F. Dijkman, J. Fluid Mech., vol. 139, pp 173-191 (1984)
- [10] J.F. Dijkman and A. Pierik, Dynamics of Piezoelectric Print-Heads, Chapter 3 of Inkjet Technology for Digital Fabrication, Edited by I.M. Hutchings and G.D. Martin, Wiley (2013), pp 60-66.
- [11] J.F. Dijkman, P.C. Duineveld, M.J.J. Hack, A. Pierik, J. Rensen, J.-E. Rubingh, I. Schram and M.M. Vernhout, J. Mater. Chem., 17, 511-522 (2007).
- [12] T. Driessen and R. Jeurissen, Fundamentals of Inkjet Printing edited by S.D. Hoath, chapter 4, Wiley-VCH (2016) pp 93-114.
- [13] A.R. Plastino and J.C. Muzzio, Celestial Mechanics and Dynamical Astronomy 53, 227-232 (1992)
- [14] M. Roseau, Vibrations non-linéaires et théorie de la stabilité, Springer Tracts in Natural Philosophy, vol. 8 (1966), Chapitre 2.
- [15] J. de Jong, G. de Bruin, H. Reinten, M. van den Berg, H. Wijshoff, M. Versluis and N. de Jong and D. Lohse, "Acoustical and Optical Characterisation of Air Entrapment in Piezo Driven Inkjet Printheads", Proceedings IEEE Ultrasonics 2, 1270-1271 (2005).
- [16] J. de Jong, R. Jeurissen, H. Borel, M. van den Berg, M. Versluis, H. Wijshoff, A. Prosperetti, H. Reinten and D. Lohse, "Entrapped air bubbles in piezo-driven inkjet printing: Their effect on the droplet velocity", Phys. Fluids 18, 121511, pp1-7 (2006).
- [17] J. de Jong, "Air entrapment in piezo inkjet printing", Dissertation Twente University 2007.
- [18] K.-S. Kwon, H.-S. Kim, M. Choi, Review of Scientific Instruments 87 (3): 035101 March 2016
- [19] S.D. Hoath, Multi-Pulse Train Modelling of Piezo DoD Inkjet Print-Head Response, to be published in JIST

Author Biography

J. Frits Dijkman obtained his masters in mechanical engineering at the Technical University of Delft in The Netherlands in 1973. He finished his PhD within the groups of Professor. D. de Jong and Professor W.T. Koiter (Technical University of Delft, The Netherlands, 1978) focussing on the engineering mechanics of leaf spring mechanisms. He worked with Philips Research Laboratories in Eindhoven, The Netherlands for 32.5 years, mainly on inkjet printing, from the basic understanding of these devices to applying the technology to display manufacturing and bio-printing. After his retirement he continued his work as part time professor at the University of Twente, The Netherlands. The topics include inkjet printing of viscoelastic inks, design of inkjet print heads and printed biosensors. He also acts as a consultant for ASML, Philips and other companies.

Email: j.f.dijkman@utwente.nl